Electron-impact excitation of silver

S. D. Tošić,[1] V. Pejčev,[1] D. Šević,[1] R. P. McEachran,[2] A. D. Stauffer,[3] and B. P. Marinković[1]
[1]*Institute of Physics, University of Belgrade, Pregrevica 118, 11080 Belgrade, Serbia*
[2]*Research School of Physical Sciences and Engineering, Australian National University, Canberra, Australian Capital Territory 0200, Australia*
[3]*Department of Physics and Astronomy, York University, Toronto, Ontario, Canada M3J 1P3*
(Received 23 March 2015; published 11 May 2015)

We measure the differential cross sections (DCSs) for the electron-impact excitation of the combined (two fine-structure levels) resonant $4d^{10}5p\ ^2P_{1/2,3/2}$ and $4d^9 5s^2\ ^2D_{5/2}$ states in silver from the $4d^{10}5s\ ^2S_{1/2}$ ground state. A comparison with the predictions of the relativistic distorted-wave (RDW) approximation model is carried out. Relativistic distorted-wave calculations are performed for each level separately and are combined to compare with the measurements. Both the experimental and theoretical results are obtained at incident electron energies E_0 of 10, 20, 40, 60, 80, and 100 eV and scattering angles θ from 10° up to 150° (experiment) and from 0° to 180° (calculations). Absolute values for the experimental DCSs are obtained by normalizing relative DCSs to theoretical RDW results at 40° at all energies except at 10 eV, where we performed the normalization of the relative DCSs at 10° to our previous small-angle experimental DCS values [S. D. Tošić *et al.*, Nucl. Instrum. Methods Phys. Res. Sect. B **279**, 53 (2012)]. The integrated cross sections, which include integral Q_1, momentum transfer Q_M, and viscosity Q_V cross sections, are determined by numerical integration of the absolute DCSs.

DOI: 10.1103/PhysRevA.91.052703 PACS number(s): 34.80.Dp

I. INTRODUCTION

This work is part of our project on electron-impact excitation of silver atoms in the medium- and low-energy regimes. Recently, we published the results of a combined experimental and theoretical study for the electron-impact excitation of the resonant $4d^{10}5s \rightarrow 4d^{10}5p$ transition in the silver atom in the intermediate electron energy range from 10 to 100 eV at small scattering angles [1]. The comparison with the relativistic distorted-wave (RDW) calculations shows good agreement between experiment and theory especially at higher energies and smaller scattering angles. We are not aware of previous experiments on the angle dependences of the DCSs in the energy range considered here that we can compare to the present work. Even if we include theoretical investigations, there are limited results reported of this scattering process (see [1] and references therein).

The purpose of the present study is to provide reliable electron scattering data that are crucial for a better understanding of electron interactions with silver atoms as well as for many scientific and practical applications [1]. The silver atom is important in the field of laser cooling and trapping techniques and therefore it is an interesting candidate for a neutral-atom-based optical frequency standard. The resonant $4d^{10}5p\ ^2P_{1/2,3/2}$ state, which is the main goal of the present investigation, is a fine-structure doublet with total angular momenta of $J = 1/2$ and $3/2$ and energies of 3.664 and 3.778 eV, respectively, and it is well suited for laser spectroscopic studies. Carlsson *et al.* [2] have measured the lifetimes of these states with high accuracy by time-resolved laser spectroscopy using the delayed coincidence technique, while Uhlenberg *et al.* [3] have performed high-resolution spectroscopic measurements of the $4d^{10}5s\ ^2S_{1/2} \rightarrow 4d^{10}5p\ ^2P_{3/2}$ cooling transition. Generally, the lifetimes of the $5p\ ^2P_{1/2}$ and $5p\ ^2P_{3/2}$ states in silver are among the most accurately known of all atomic lifetimes. Comparing other possible systems such as Ca, Rb, Sr, Yb, and Cs used as optical frequency standards that are based on optically probed electronic transition, usually a forbidden transition, with narrow bandwidth, there has been some interest in silver using a transition between the $4d^{10}5s\ ^2S_{1/2}$ ground state and the metastable $4d^9 5s^2\ ^2D_{5/2}$ level, which is an extremely narrow transition with a small natural linewidth (≈0.8 Hz). Larkins and Hannaford [4] have determined the energy of the $4d^9 5s^2\ ^2D_{5/2}$ metastable level and the frequency of the transition. Badr *et al.* [5] presented a detailed description of this optical two-photon excitation process and determined the frequency, hyperfine coupling constants, and isotope shift of this transition. This metastable state is important in terms of our present investigation since its energy of 3.749 eV lies between the combined resonant $4d^{10}5p\ ^2P_{1/2,3/2}$ states and its contribution to the DCS could not be distinguished in experimental energy-loss spectra at the present energy resolution. Theoretically, each of these lines can be calculated separately and combined as required.

Here we present experimental and theoretical investigations of electron excitation of the silver atom from the ground state to the resonant line $4d^{10}5p$ at impact energies from 10 to 100 eV. The present investigations are now extended over a wide range of scattering angles up to 150° for experiment and up to 180° for theory. The normalized experimental DCS values were extrapolated to 0° and 180° following the guidance of calculations and were numerically integrated in order to obtain the integral Q_1, momentum transfer Q_M, and viscosity Q_V cross sections. Relativistic distorted-wave calculations were performed for both fine-structure levels and combined to compare with the measurements.

This paper is organized as follows. The experimental technique and procedure are described in Sec. II. In Sec. III the RDW method is outlined. The results are shown and discussed in Sec. IV. A summary is given in Sec. V.

II. EXPERIMENTAL TECHNIQUES AND PROCEDURES

The apparatus used in this experiment is a conventional crossed-beam electron spectrometer especially designed for

 ©2015 American Physical Society

electron–metal-atom investigations that has been described in detail earlier [1,6–11]. In this crossed-beam arrangement binary collisions are favored, the density of target particles is small enough to ensure that an incident electron interacts with only one target particle, and the density of the electron beam is low enough to ensure that the electrons do not interact with each other. Briefly, the experimental apparatus consists of a hemispherical electron energy selector with a hairpin thermoelectron source in order to provide a monoenergetic electron beam and an energy analyzer of the same type (two hemispheres of identical dimensions to the monochromator) equipped with a channel electron multiplier as a detector in order to analyze and detect the inelastically scattered electrons. The analyzer can be positioned from $-30°$ up to 150° with respect to the zero angle defined by the axis of the electron beam.

The vacuum chamber also contains an oven as a source of the atomic beam. A silver vapor beam was produced by heating a Knudsen-type crucible by two separate coaxial heaters. In this way the top and the bottom of the crucible can be independently heated and temperature gradients of approximately 100 K needed to avoid clogging were achieved (the top of the system was maintained at a higher temperature than the bottom). The stability of the oven's temperature was controlled and monitored by two thermocouples, one installed at the top of the crucible and the second at the bottom. The measurements were performed at a working temperature of about 1300 K. Water cooling, additional shields, and a liquid-nitrogen cold trap located above the oven and interaction region prevented contamination of the vacuum chamber from the Ag vapor and overheating of surrounding components. In order to achieve better compensation for the earth's magnetic field, the vacuum chamber was shielded by a double μ-metal shield and the measured magnetic field at the position of the interaction volume was below 2×10^{-7} T. The vacuum inside the chamber was provided by two diffusion pumps and a background pressure of the order of 10^{-5} Pa was maintained.

The overall energy resolution (full width at half maximum) of the energy-loss spectra was typically 160 meV, while the angular resolution was 1.5°. The position of the true zero scattering angle was determined before each angular distribution measurement by checking the symmetry of the scattered electrons at negative and positive scattering angles (from $-10°$ to $+10°$). The scattered electron intensities were recorded in the accessible angular range at the fixed energy loss that corresponds to the excitation energy of the resonance transition. Due to the change of effective interaction volume versus scattering angle, the effective path length correction factors $V_{\rm eff}$ [12] determined for the present experimental conditions were applied and the corrections of measured scattered intensities were made. Before each measurement the energy-loss spectrum was accumulated in order to check the stability of the target beam and to verify the absence of double scattering. No structures that correspond to the residual background gas were observed. The relative DCSs obtained at 20, 40, 60, 80, and 100 eV were put on an absolute scale by normalization to the RDW values calculated at 40°. This scattering angle of 40° was chosen for normalization since the signal intensities at this angle are relatively large compared to those at larger scattering angles, while the influence of the effective path length correction factor is relatively small at small angles. Absolute DCSs at 10 eV were obtained by normalization to the absolute DCSs for the same excitation

TABLE I. Differential cross sections, in units of 10^{-20} m^2 sr^{-1}, for electron excitation of the $4d^{10}5p\ ^2P_{1/2,3/2}$ levels of silver. The numbers in parentheses are absolute uncertainties. The extrapolated values are given in square brackets. The last three lines are integral $Q_{\rm I}$, momentum transfer $Q_{\rm M}$, and viscosity $Q_{\rm V}$ cross sections obtained by integrating our measured DCS in units of 10^{-20} m^2.

Angle (deg)	Energy (eV)					
	10	20	40	60	80	100
10	30.9(3.2)	27.4(2.8)	14.3(2.5)	7.3(1.5)	4.8(1.2)	1.95(59)
20	10.2(3.0)	5.7(1.7)	1.85(55)	0.47(14)	0.35(11)	0.168(34)
30	1.89(57)	1.54(46)	0.222(66)	0.114(34)	0.155(46)	0.097(19)
40	0.39(12)	0.59(18)	0.073(22)	0.048(14)	0.071(21)	0.065(13)
50	0.130(39)	0.159(48)	0.051(15)	0.0222(66)	0.0277(83)	0.0293(59)
60	0.096(29)	0.047(19)	0.039(12)	0.0085(34)	0.0083(25)	0.0111(22)
70	0.055(16)	0.0189(75)	0.047(14)	0.0050(20)	0.0144(43)	0.0129(26)
80	0.0290(87)	0.0216(86)	0.026(11)	0.0052(21)	0.0155(46)	0.0148(45)
90	0.0190(57)	0.049(19)	0.0211(95)	0.0061(18)	0.0194(58)	0.0133(40)
100	0.0149(45)	0.0235(70)	0.045(13)	0.0120(36)	0.0066(33)	0.0072(21)
110	0.0033(16)	0.0194(58)	0.074(22)	0.0161(48)	0.0039(19)	0.0033(13)
120	0.0043(21)	0.037(11)	0.122(37)	0.0205(61)	0.00277(97)	0.0053(21)
130	0.0053(19)	0.044(13)	0.058(17)	0.0149(45)	0.00277(97)	0.0061(24)
140	0.0071(25)	0.047(14)	0.103(31)	0.0040(12)	0.00195(68)	0.00297(89)
150	0.040(14)	0.220(66)	0.144(43)	0.0041(12)	0.0033(12)	0.0075(22)
160	[0.03998]	[0.33047]	[0.46313]	[0.02323]	[0.01333]	[0.02668]
170	[0.04014]	[0.42993]	[0.80877]	[0.04753]	[0.02552]	[0.04923]
180	[0.04026]	[0.471]	[0.95841]	[0.05863]	[0.03104]	[0.05941]
$Q_{\rm I}$	12.4(4.7)	11.2(3.8)	6.8(2.8)	4.5(2.0)	3.3(1.8)	3.0(1.9)
$Q_{\rm M}$	3.3(1.4)	2.4(1.1)	1.81(96)	0.35(18)	0.23(13)	0.22(12)
$Q_{\rm V}$	5.4(2.2)	3.1(1.2)	1.25(62)	0.46(23)	0.33(19)	0.26(15)

process at 10° [1]. Then the absolute DCSs were extrapolated to 0° and 180° and numerically integrated to yield integral Q_I, momentum transfer Q_M, and viscosity Q_V cross sections [Eqs. (1)–(3) in [7]]. Extrapolation of the DCS to 0° was made using the measured results at small scattering angles [1]. For extrapolation to 180° we used the RDW calculations for the given energy.

III. THEORY

Electron-impact excitation of the silver atom is expected to show relativistic effects. In heavy and moderately heavy atoms such as silver ($Z = 47$), these effects are manifested in the fine-structure splitting of the excited states. The RDW method formulated by Zuo *et al.* [13] includes both the fine structure of the atom and the spin-orbit coupling of the scattered electrons and was used for the calculation of the excitation processes in many electron-atom systems [7,14–17] including the electron-silver excitation [1,18]. In the present study we extend the RDW method to the electron excitation of the $4d^{10}5p$ states of silver (a fine-structure doublet with the lower level having $J = 1/2$ and the upper level $J = 3/2$ with an energy splitting of 0.114 eV). Since we have already used this method for the same process at small scattering angles, the details of the calculation method are given in [1] and references therein. We calculated differential cross sections for each level separately and the combined results were compared with the measurements.

IV. RESULTS AND DISCUSSION

Differential cross sections for the electron excitation of the $4d^{10}5p\ ^2P_{1/2,3/2}$ states of silver were measured for scattering angles ranging from 10° to 150° and at intermediate electron-impact energies of 10, 20, 40, 60, 80, and 100 eV. Relativistic distorted-wave calculations were performed at the same energies and scattering angles up to 180°. The DCSs were also integrated over all angles and thus integrated cross sections were obtained. All results are presented in Table I and summarized in Figs. 1–5. The extrapolated experimental values obtained by using the normalized shape of the RDW cross sections are also given in Table I. See Supplemental Material in [19] for the numerical data from the RDW calculations.

The electron excitation of the silver atom is presented in an electron-energy-loss (EEL) spectrum at 40 eV impact energy and at a scattering angle of 10° as shown in Fig. 1. The energy range covered by this spectrum was adjusted to include the region below the first ionization limit of 7.576 eV [20] and the autoionization region up to 9.2 eV. The assignment of atomic energy states is given by using the results on the NIST website [21]. The low-energy region of this spectrum is dominated by an intense feature at about 3.7 eV that is due to the electron excitation of the $4d^{10}5p\ ^2P_{1/2,3/2}$ fine-structure levels (our energy resolution was not high enough to resolve these two states). It is also evident that this structure is

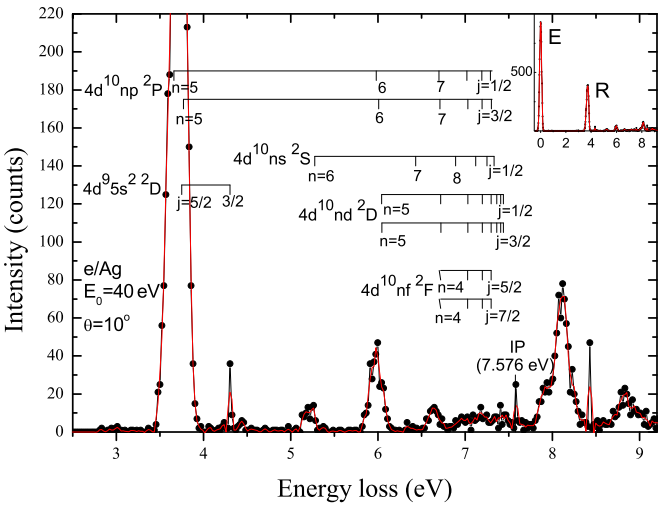

FIG. 1. (Color online) Energy-loss spectrum of silver at 40 eV electron-impact energy and 10° scattering angle. The energy-loss spectrum with features that correspond to the elastic scattering E and to the resonant excitation R is shown in the inset. Closed circles denote the measured intensity and the solid line shows the best fit.

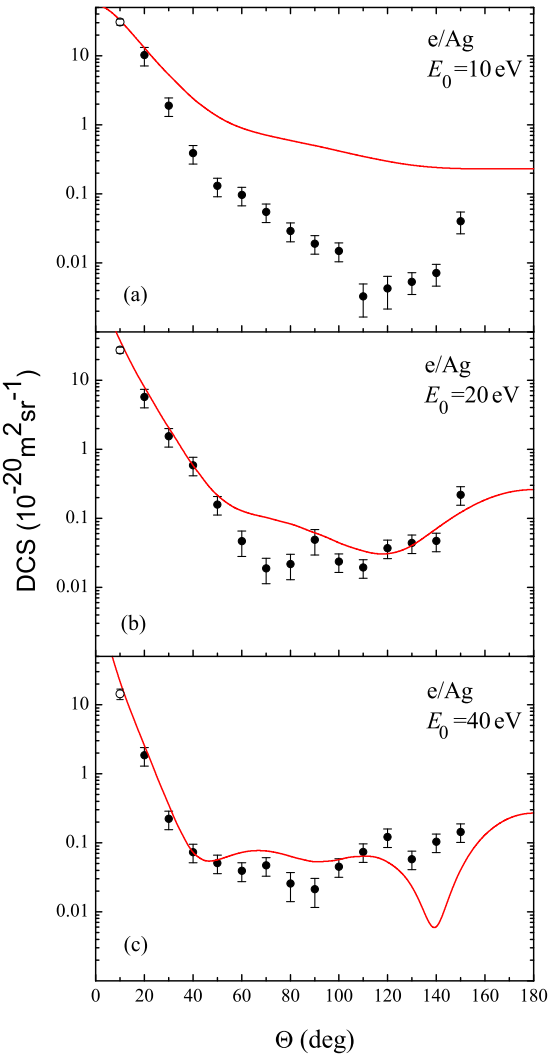

FIG. 2. (Color online) Differential cross sections for the $4d^{10}5p\ ^2P_{1/2,3/2}$ excitation of silver at (a) 10 eV, (b) 20 eV, and (c) 40 eV electron-impact energies. Closed circles denote the present experimental results with uncertainties. The solid line shows the DCSs calculated by the RDW method for the combined levels.

clearly resolved from the other ones in the EEL spectrum including the feature that corresponds to elastic scattering (see the inset in Fig. 1). Also, the intensities of other peaks (each characteristic of a particular allowed or forbidden transition) are significantly smaller than that of the unresolved silver resonant line. The position of the $4d^9 5s^2\ ^2D_{5/2}$ metastable state with an energy of 3.749 eV lies between the $4d^{10}5p\ ^2P_{1/2}$ state at 3.664 eV and the $4d^{10}5p\ ^2P_{3/2}$ state at 3.778 eV. However, since the excitation from the ^2S ground state to the $^2D_{5/2}$ level is not a dipole-allowed transition (it decays by electron quadrupole radiation), we assume that its contribution to the measured excitation cross sections of the resonance ^2P states is negligible.

Figure 2 presents both the measured and calculated DCSs at electron-impact energies of 10, 20, and 40 eV. All DCSs are strongly forward peaked as is typical of a dipole-allowed transition. The experimental 10-eV data [Fig. 2(a)] exhibits a structure at 50° (inflection point) and one relatively deep minimum at 110°. There is an abrupt decrease in the cross section between 100° and 110° as well as a jump between 140° and 150°. This behavior was consistent in all data sets obtained at this particular impact energy. The data at 20 eV [Fig. 2(b)] exhibit the presence of two minima, one at 70° and the other at the same angle of 110° as at 10 eV, while the local maximum is at 90°. Again, the cross section increases significantly between 140° and 150°. The DCS at an electron energy of 40 eV [Fig. 2 (c)] decreases markedly up to 40°, the minimum is located at 90°, and then the DCS values increase as the scattering angle increases.

At 10 eV, the incident electron energy is too low for the RDW method to produce reliable results and there is agreement with the measurements only at angles below 20° (which is due to the normalization of the small scattering angle DCS to the RDW data at 5° [1]). At higher angles the experiment gives significantly smaller DCS values but with more structures in the shape. At 20 eV the RDW calculations are in better agreement but do not show the minimum around 70° seen in our measurements. At larger scattering angles they exhibit a shallow minimum near 120°, while the experiment has a deeper minimum around 110°. For 40 eV we observe good agreement in shape between the present experimental and the RDW results at angles up to 110°, though the values obtained from the measurements are lower than from 60°–90°, while at higher scattering angles the calculated DCSs show a deep minimum at 140° in contrast to the shallow experimental one observed at 130°.

The calculated DCSs for the excitation of the $4d^{10}5p\ ^2P_{1/2}$ and $4d^{10}5p\ ^2P_{3/2}$ states of Ag, as well as the differential

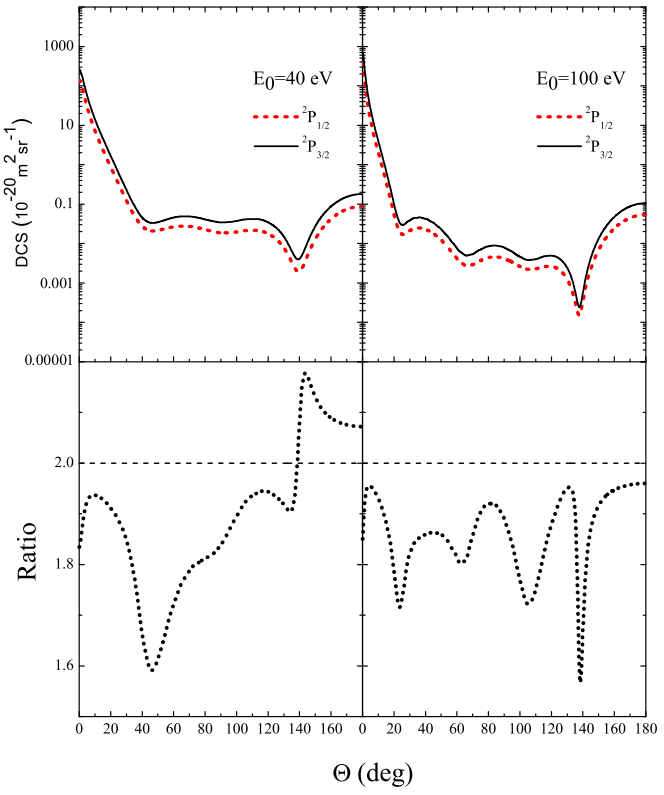

FIG. 3. (Color online) (a) Calculated differential cross sections for the $4d^{10}5p\ ^2P_{1/2}$ (dashed line) and $4d^{10}5p\ ^2P_{3/2}$ (solid line) excitations of silver and (b) differential branching ratios of the $4d^{10}5p\ ^2P_{1/2,3/2}$ states of Ag at 40 and 100 eV.

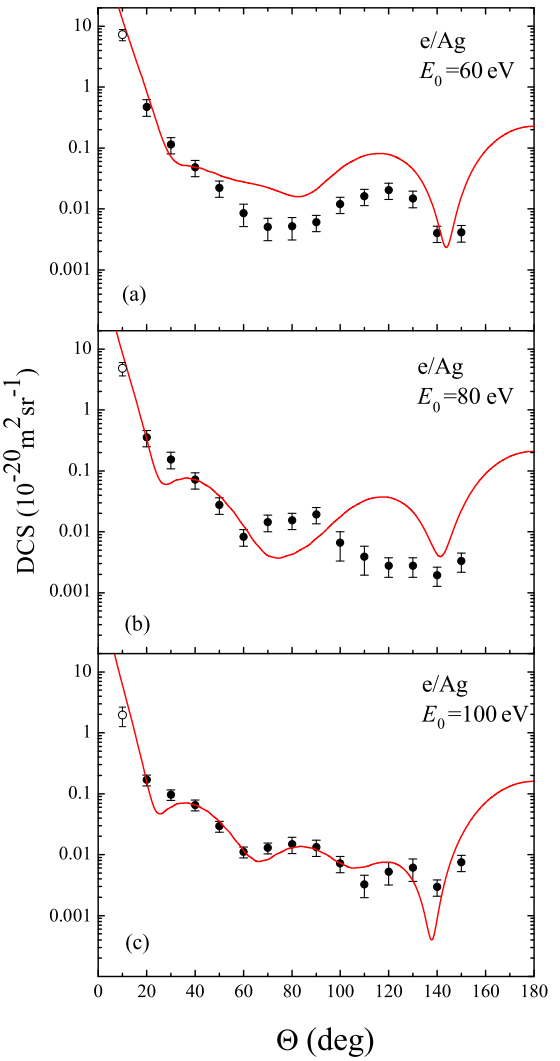

FIG. 4. (Color online) Same as for Fig. 2 except for (a) 60 eV, (b) 80 eV, and (c) 100 eV electron-impact energies.

branching ratios $DCS_{3/2}/DCS_{1/2}$ at 40 and 100 eV electron-impact energies, are shown in Fig. 3. The results show that there are no noticeable differences in the shape of the cross-section data for $^2P_{1/2}$ and $^2P_{3/2}$ states, but the differential branching ratios show deviations from the fine-structure approximation value of 2 (Eq. 4 in [18]). Zeman *et al.* [18] have also found that this branching ratio deviates significantly from 2 at 30, 50, and 100 eV electron-impact energies, which indicates the existence of relativistic effects in silver atoms. These ratios show significant deviations from 2, ranging from 1.6 to 2.2 at 40 eV, and are primarily associated with the fact that the extrema occur at slightly different angles for the two fine-structure levels. This is particularly apparent at 100 eV, where there are several extrema in the calculated cross sections.

Differential cross-section results at 60, 80, and 100 eV are presented in Fig. 4. At an electron energy of 60 eV [Fig. 4(a)], both the measured and calculated curves have similar shapes over the whole angular range, though the theoretical results are somewhat larger at angles greater than 50° except in the vicinity of a deep minimum at 144°. At 80 eV [Fig. 4(b)] the agreement between experiment and the RDW calculations is quite good at angles below 60°. However, above this angle the measurements show a broad maximum followed by a minimum, whereas the calculated DCSs have the opposite behavior except for the pronounced minimum at 143°, which approaches the measured value. The RDW calculations at 100 eV [Fig. 4(c)] agree quite well with the shape and absolute values of the experimental DCSs. However, there is some difference in magnitude in the region of the two higher minima.

The three-dimensional (3D) profile of the differential cross sections as a function of electron-impact energy and scattering angle is shown in Fig. 5. The figure clearly shows the position of the measured DCSs with respect to the calculated values. Strong forward peaked behavior at small scattering angles

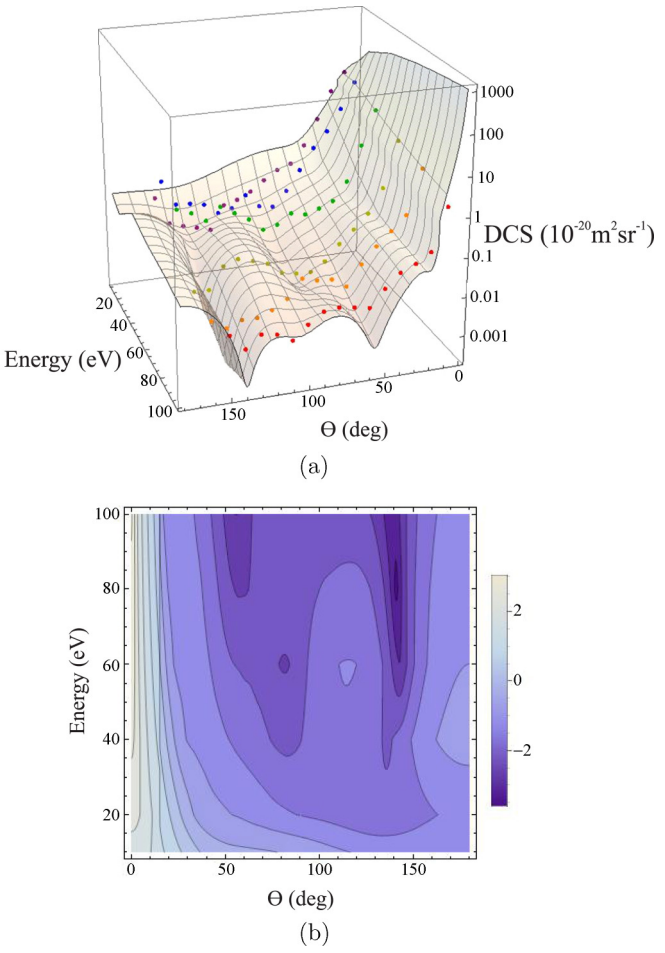

FIG. 5. (Color online) (a) The 3D profile of the differential cross sections as a function of electron-impact energy and scattering angle. Closed circles denote the present experimental results. The surface is made using the RDW data. (b) Contour plot of the RDW data. The vertical axis represents the electron-impact energy (in eV), while the horizontal axis represents the scattering angle (in degrees). The contour lines for the DCS are incremented in powers of 10 according to the legend on the right-hand side of the plot in units of 10^{-20} m^2 sr^{-1}.

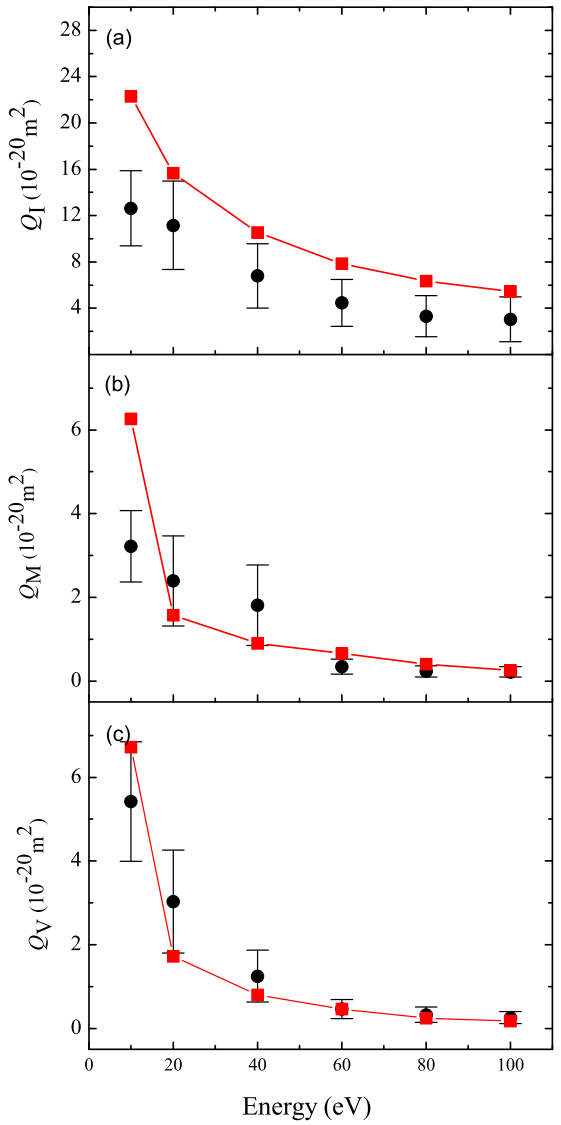

FIG. 6. (Color online) (a) Integral, (b) momentum transfer, and (c) viscosity cross sections for electron-impact excitation of the $4d^{10}5p\ ^2P_{1/2,3/2}$ state of silver. The experimental points are the same as for Figs. 2 and 4. The solid lines with squares show the ICSs calculated by the RDW method for the combined levels.

characterizes the cross sections of the present transitions. The 3D surface shows a prominent valley near 140°, though the other structures are not as well defined.

In Fig. 6 we present the results for the integral Q_{I} [Fig. 6(a)], momentum transfer Q_{M} [Fig. 6(b)], and viscosity Q_{V} [Fig. 6(c)] cross sections for electron excitation of the combined $4d^{10}5p\ ^2P_{1/2,3/2}$ levels of silver. The formulas for these were given in [7]. At all electron energies, extrapolation of the experimental DCSs to 0° was based on the small-angle measurements [1], while extrapolation to 180° was made using the RDW calculated DCS profiles. The measurements confirm a monotonic decrease of Q_{I}, Q_{M}, and Q_{V} with increasing incident electron energy as is also predicted by theory. Reasonably good agreement was achieved between experiment and theory concerning the shape of the energy dependences of all integrated cross sections, but theory gives slightly larger values of the integral cross sections at all electron energies. The main reason for this behavior is the fact that the present calculated DCSs are higher than the normalized measured ones over the whole angular range. For the momentum transfer and viscosity cross sections the calculated cross sections lie at the lower limits of the measured uncertainties at 20 and 30 eV, while there is closer agreement with the measurements at higher energies, especially for the viscosity cross sections.

It is assumed that the contribution of the $4d^95s^2\ ^2D_{5/2}$ excitation to the measured scattered electron intensities can be neglected. Although the excitation of the optically forbidden states by electron impact will occur, the DCS for these excitations is small compared with the DCS for the resonant excitation. This is illustrated in Fig. 1, where the signal from the $J = 3/2$ state is much smaller than that for the resonant excitation. Since the DCS for excitation of the $J = 5/2$ state will have the same magnitude, it can be ignored in the present measurements. Calculations are needed to provide a quantitative value for these DCSs. Also, as we already reported in our previous paper [1], the DCS for the combined levels can be represented as a sum of the DCSs for the excitation of the individual fine-structure levels.

V. CONCLUSION

This paper has reported the results of experimental and theoretical studies of the electron-impact excitation of the $4d^{10}5p$ state of silver at intermediate energies and for the full range of scattering angles. Experimental methods based on a crossed-beam technique as well as the apparatus employed were described. Calculations were carried out using the relativistic distorted-wave method. Differential and integrated cross sections were obtained at electron energies of 10, 20, 40, 60, 80, and 100 eV and scattering angles from 10° to 150° in the experiment, while the calculations cover the full angular range. Reasonable agreement was achieved between the present two sets of data at energies of 20 eV and above.

We are not aware of experimental data that we can compare to the present work. It would be interesting and important to continue investigations on this excitation process in order to obtain a more profound knowledge of electron excitation processes in silver atoms and to obtained more complete sets of scattering data that could be used in further modeling.

ACKNOWLEDGMENTS

This work was supported by the Ministry of Education, Science and Technological Development of Republic of Serbia (Project No. OI 171020) and was conducted within the framework of the COST Action CM1301 (CELINA). We are grateful to A. Bunjac for technical support.

[1] S. D. Tošić, V. Pejčev, D. Šević, R. P. McEachran, A. D. Stauffer, and B. P. Marinković, Absolute differential cross sections for electron excitation of silver at small scattering angles, Nucl. Instrum. Methods Phys. Res. Sect. B **279**, 53 (2012).

[2] J. Carlsson, P. Jonsson, and L. Sturesson, Accurate time-resolved laser spectroscopy on silver atoms, Z. Phys. D **16**, 87 (1990).

[3] G. Uhlenberg, J. Dirscherl, and H. Walther, Magneto-optical trapping of silver atoms, Phys. Rev. A **62**, 063404 (2000).

[4] P. L. Larkins and P. Hannaford, Precision measurement of the energy of the $4d^95s^2\ ^2D_{5/2}$ metastable level in Ag I, Z. Phys. D **32**, 167 (1994).

[5] T. Badr, M. D. Plimmer, P. Juncar, M. E. Himbert, Y. Louyer, and D. J. E. Knight, Observation by two-photon laser spectroscopy of the $4d^{10}5s\ ^2S_{1/2} \rightarrow 4d^95s^2\ ^2D_{5/2}$ clock transition in atomic silver, Phys. Rev. A **74**, 062509 (2006).

[6] S. Milisavljević, M. S. Rabasović, D. Šević, V. Pejčev, D. M. Filipović, L. Sharma, R. Srivastava, A. D. Stauffer, and B. P. Marinković, Electron-impact excitation of the $6p7s\ ^3P_1$ state of Pb atom at small scattering angles, Phys. Rev. A **75**, 052713 (2007).

[7] S. Milisavljević, M. S. Rabasović, D. Šević, V. Pejčev, D. M. Filipović, L. Sharma, R. Srivastava, A. D. Stauffer, and B. P. Marinković, Excitation of the $6p7s\ ^3P_{0,1}$ states of Pb atoms by electron impact: Differential and integrated cross sections, Phys. Rev. A **76**, 022714 (2007).

[8] S. D. Tošić, M. S. Rabasović, D. Šević, V. Pejčev, D. M. Filipović, L. Sharma, A. N. Triphati, R. Srivastava, and B. P. Marinković, Elastic electron scattering by a Pb atom, Phys. Rev. A **77**, 012725 (2008).

[9] M. S. Rabasović, V. I. Kelemen, S. D. Tošić, D. Šević, M. M. Dovhanych, V. Pejčev, D. M. Filipović, E. Yu. Remeta, and B. P. Marinković, Experimental and theoretical study of the elastic-electron–indium-atom scattering in the intermediate energy range, Phys. Rev. A **77**, 062713 (2008).

[10] B. P. Marinković, V. Pejčev, D. M. Filipović, D. Šević, S. Milisavljević, and B. Predojević, Electron collisions by metal atom vapours, Rad. Phys. Chem. **76**, 455 (2007).

[11] S. D. Tošić, V. I. Kelemen, D. Šević, V. Pejčev, D. M. Filipović, E. Y. Remeta, and B. P. Marinković, Elastic electron scattering by silver atom, Nucl. Instrum. Methods Phys. Res. Sect. B **267**, 283 (2009).

[12] R. T. Brinkman and S. Trajmar, Effective path length corrections in beam-beam scattering experiments, J. Phys. E **14**, 245 (1981).

[13] T. Zuo, R. P. McEachran, and A. D. Stauffer, Relativistic distorted-wave calculation of electron impact excitation of xenon, J. Phys. B **24**, 2853 (1991).

[14] R. Srivastava, T. Zuo, R. P. McEachran, and A. D. Stauffer, Excitation of the $^{1,3}P_1$ states of calcium, strontium and barium in the relativistic distorted-wave approximation, J. Phys. B **25**, 3709 (1992).

[15] V. Zeman, R. P. McEachran, and A. D. Stauffer, Relativistic distorted-wave calculation of electron impact excitation of caesium, J. Phys. B **27**, 3175 (1994).

[16] R. Srivastava, V. Zeman, R. P. McEachran, and A. D. Stauffer, Excitation of copper by electron impact in the relativistic distorted-wave approximation, J. Phys. B **28**, 1059 (1995).

[17] S. Kaur, R. Srivastava, R. P. McEachran, and A. D. Stauffer, Excitation of thallium and lead atoms by electrons in the relativistic distorted-wave approximation, J. Phys. B **33**, 2539 (2000).

[18] V. Zeman, R. P. McEachran, and A. D. Stauffer, Relativistic distorted-wave approximation of electron impact excitation of silver and gold, Can. J. Phys. **74**, 889 (1996).

[19] See Supplemental Material at http://link.aps.org/supplemental/10.1103/PhysRevA.91.052703 for the numerical data from the RDW calculations.

[20] J. E. Sansonetti and W. C. Martin, Handbook of basic atomic spectroscopic data, J. Phys. Chem. Ref. Data **34**, 1559 (2005).

[21] A. Kramida, Yu. Ralchenko, J. Reader, and NIST ASD Team, NIST Atomic Spectra Database, version 5.2, available at http://physics.nist.gov/asd (National Institute of Standards and Technology, Gaithersburg, 2014).